The impact of greenhouse gases, regions, and sectors on future temperature anomaly with the FaIR model

Tej Kosaraju[1], Paul Griffiths[2]
[1] Adlai E. Stevenson High School, Lincolnshire, Illinois
[2] Centre for Atmospheric Science, University of Cambridge, Cambridge, United Kingdom

SUMMARY
Greenhouse gas emissions from industrial activities have resulted in global warming, threatening the human way of life. Climate modeling is crucial to the effort to combat climate change by determining the potential impacts of anthropogenic emissions and thus identifying where emission reduction efforts should focus. In this study, we hypothesized that various economic sectors, geographic regions, and greenhouse gas species could impact the future global mean surface temperature (GMST) anomaly in ways that deviate from the historical and present norm. We used the Finite Amplitude Impulse Response (FaIR) model, a reduced complexity climate model, as well as four of the Shared Socioeconomic Pathways (SSPs), SSP126, SSP245, SSP370 and SSP585, to test our hypothesis. We determined that the future impact of specific economic sectors, geographic regions, and greenhouse gas species deviates from their historical impact. We found that Asia and Africa will contribute to a greater share of the GMST anomaly in the future. We also determined that the warming from most of the greenhouse gas species, excluding carbon dioxide, is highest under the SSP370 scenario (the climate scenario that emphasizes regional rivalries related to climate policy). We concluded that the industrial sector would become more important under the SSPs that represent a lower degree of warming. This research augments the SSPs by considering specific variables not represented in the general SSP scenarios, determining the precise climate impacts of said variables. Additionally, this research helps to determine what emission reduction strategies can most efficiently reduce the GMST anomaly.

INTRODUCTION
The warming effect known as the Greenhouse Effect is the result of anthropogenic gases being released into the troposphere, primarily by the burning of fossil fuels. These greenhouse gases are atmospheric compounds that absorb and radiate long wave electromagnetic radiation. After shortwave radiation from the sun hits the Earth, some of it is reflected in the form of longwave radiation (1). This is crucial to the existence of life on the planet, raising the global mean surface temperature (GMST) by 15°C on average. However, in recent years, anthropogenic emissions of greenhouse gases are resulting in an increased warming effect that is disrupting human activities (2).

The climate science field has long recognized the need for scenario sets, or projections that connect socioeconomic and political trends to emissions in order to analyze the potential future GMST trends. For this reason, a group of climate scientists developed the Representative Concentration Pathways (RCPs) for use in the Intergovernmental Panel on Climate Change's (IPCC's) 5th Assessment Report (AR5). These pathways aimed to summarize existing literature and created four different emissions trajectories representing specific climate scenarios. These pathways were based on the effective radiative forcing (ERF) which is defined as the net (incoming minus outgoing) radiative flux at the top of Earth's atmosphere following a perturbation to atmospheric composition, such as the increase in a greenhouse gas species (3). ERFs are the IPCC's preferred method to connect radiative forcing to GMST changes, with a positive forcing corresponding to an increase in GMST. The RCPs utilized pathways with ERFs ranging from 2.6 to 8.5 Wm-2 for modeling purposes to represent the potential range of human-caused radiative forcings. (3). These RCPs, while useful for the standardization and comparison of climate models, purposefully lacked socioeconomic narratives, solely focusing on scientific criteria and thus could not be used to analyze the impact of climate policy and mitigation measures. As a result, for the 6th Assessment Report (AR6), the climate change research community created the Shared Socioeconomic Pathways (SSPs) to replace the RCPs and provide a narrative for different trends that could shape future emissions (4). These range from the SSP1 "sustainability" pathway to the SSP5 "fossil-fuel development pathway," and are the primary scenarios used today in climate modeling (4). The smaller SSPs represent better climate outcomes and less warming due to general global policy trends (**Table 1**). The SSPs are built on broad socioeconomic narratives that are then connected to specific radiative forcing and GMST ranges, creating a direct connection between climate policy and the resulting temperature impact. These pathways are instrumental as comparison points for different climate models, allowing different groups to standardize their forcing scenarios. As a result, SSPs have allowed for many different models to be used together in predictions, allowing for more confidence in projections by minimizing the flaws inherent to each model's processes. By allowing for multi-modal analysis, the SSPs have created a high complexity, high-cost modeling framework that is the gold standard for climate modeling (4).

The SSPs are now the primary pathways used in Model Intercomparison Projects, which are analyses based on the outputs of many climate models that aim to address climate science questions. SSPs are even the primary pathways used in the recent Coupled Model Intercomparison Project 6 (CMIP6), which is the worldwide collaboration of climate

https://doi.org/10.59720/24-067

modeling groups that provides the results from around 100 models for AR6. This report is the flagship paper of the United Nations (UN) Intergovernmental Panel on Climate Change (IPCC) and reflects progress in accurately cataloging historical and future emissions. Using these models, the report provides analyses of the effective radiative forcing and GMST changes caused by common greenhouse gas species and aerosols. It also used each SSP to confirm the estimated rise in GMST at the end of the century, splitting up the relative causes of warming due to carbon dioxide (CO_2), warming due to non-CO_2 greenhouse gas species, and cooling due to aerosols and land use.

The SSPs are useful due to their general nature for showcasing the consequences of delayed action but do not encompass specific emissions reduction schemes, hindering their usefulness in proactive policy decisions. As a result, they do not provide useful information about specific variables, such as the temperature impact of methane emissions from agricultural waste burning. It is therefore interesting to examine the impact of smaller-scale variables such as specific economic sectors, geographical regions, and greenhouse gas species on the future GMST anomaly (**Table 2**). The IPCC's AR6 report does identify the impact of some different greenhouse gas species, splitting up future warming coming from CO_2, a single category for all non-CO_2 greenhouse gas species, and aerosols and land use under each SSP. However, this analysis does not go into the future temperature anomalies of geographic regions, economic sections, or specific greenhouse gas species other than CO_2.

In this study, we aimed to specifically describe the impact of variables such as geographic regions, economic sectors, and greenhouse gas species which are only broadly outlined under the SSPs. The CMIP6 project incorporates the models and data from 46 modeling groups, requiring such high levels of computing power and resources that modifying these experiments further is not feasible (8). This problem has been noted by the climate modeling community and has resulted in collaboration towards many reduced complexity climate models that are calibrated to accurately emulate the modeled temperature responses to changes in emissions of various species. In this study, we have used one of these models, the Finite Amplitude Impulse Response (FaIR) model. Since the FaIR model is based on the data from the same climate models as CMIP6, it has a similar predictive power but with much lower computing power required (6). The model reproduces the CMIP6 range of temperature anomaly data, or the anomaly with respect to the pre-industrial period, through equation-based parameterizations of the response of climate forcing to emissions. As a result, we believe that FaIR was well-suited for testing our hypothesis due to its climate sensitivity and transient climate response that is in excellent agreement with the IPCC ranges (6).

Name	Socioeconomic Path	Description
SSP1-2.6	Sustainability	Limit peak warming to 2°C throughout the 21st century with a likelihood of >67%
SSP2-4.5	Middle of the Road	Limit peak warming to 3°C throughout the 21st century with a likelihood of >50%
SSP3-7.0	Regional Rivalry	Limit peak warming to 4°C throughout the 21st century with a likelihood of >50%.
SSP5-8.5	Fossil-fueled Development	Exceed warming of 4°C during the 21st century with a likelihood of ≥50%.

Table 1: The definitions of the Shared Socioeconomic Pathways (SSPs) used in GMST predictions. Descriptions, socioeconomic paths, and official names are from the IPCC AR6 report (5).

Region Name	Description
ASIA	The emissions of most Asian countries with the exception of the Middle East, Japan, and the Former Soviet Union States
LAM	The emissions from Latin America and the Caribbean
REF	The emissions from the reforming economics of Eastern Europe and the Former Soviet Union
MAF	The emissions from the Middle East and Africa
OECD	The Organization for Economic Co-operation and Development (OECD 90) countries as well as EU 358 member states and candidates

Table 2: The definitions of the regions used for emission calculations in this paper. Descriptions and region names are from the RCMIP project (9).

We used this model to determine how much of an impact specific economic sectors, geographic locations, and greenhouse gas species could have on future GMST anomalies. Here we use "species" as defined in the FaIR model, to refer to the anthropogenic gases and aerosols that are involved in the calculation of radiative forcing and GMST change (6). Each experiment represents the removal, or 'zeroing out', of the emissions of a specific species, sectors, and/or region. For example, one model removes the emissions of methane from the industrial sector from its predictions. By comparing with the original FaIR experiment for the SSP, the change in GMST anomaly that resulted from the specified emissions change was determined, under the given baseline conditions of each SSP. The difference in GMST anomaly between the experiment and the baseline was identified with the warming/cooling attributable to the sector/species/region of interest.

In this study, we hypothesized that various economic sectors, geographic regions, and greenhouse gas species could impact the future global mean surface temperature anomaly in ways that deviate from the historical and present norm. We determined that one scenario (SSP370) is of concern due to its higher anomaly for many non-CO_2 species, and that the industrial sector for CO_2 will become much more important under SSPs with less warming.

RESULTS

To better understand where emission reductions should occur under the four standardized climate modeling SSPs, we looked at the GMST anomaly caused by the emissions of species in each geographical region, using region definitions from the RCMIP (Reduced Complexity Model Intercomparison Project) (**Table 1, 2**). We designed the experiments to attribute the GMST anomaly of each species to these regions and compared them across SSPs. Each subplot contains the anomaly data for each region for a single species, including a column with the total anomaly of said species (**Figure 1**). As expected, for most of the subplots, the anomaly generally increases in magnitude towards the more extreme SSPs with higher defined radiative forcings.

https://doi.org/10.59720/24-067

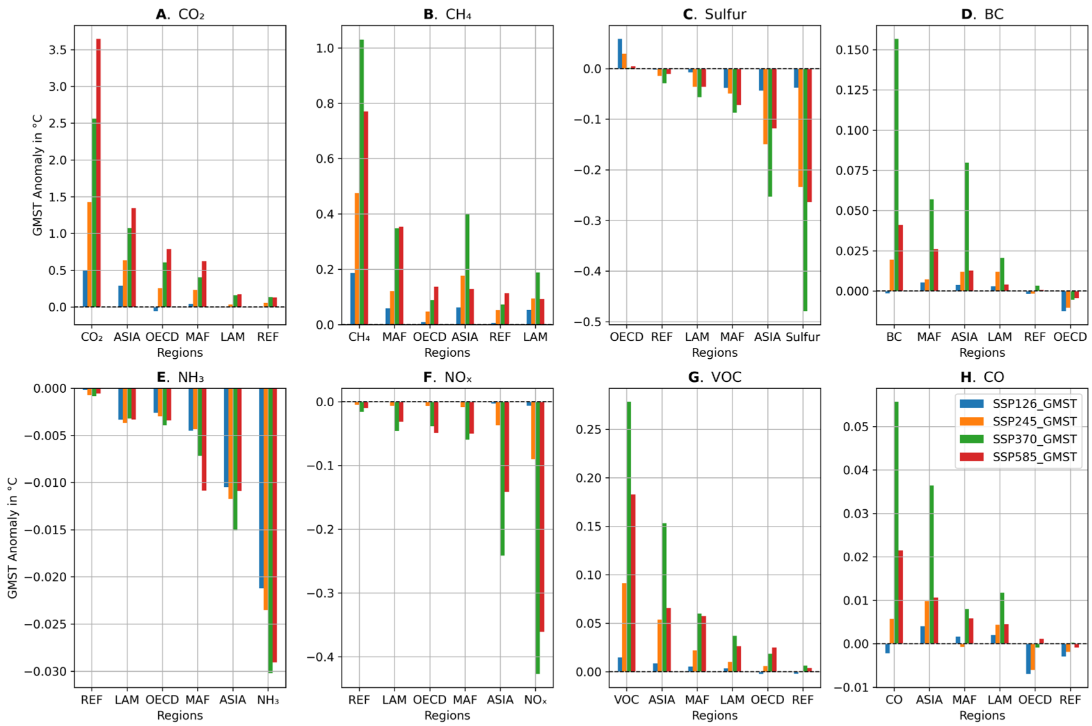

Figure 1: The predicted region-based GMST anomaly in °C under four SSPs from the Finite Amplitude Impulse Response (FaIR) model. The greenhouse gas species represented are a) carbon dioxide (CO_2), b) methane (CH_4), c) sulfur, d) black carbon (BC), e) ammonia (NH_3), f) nitrous oxides (NO_X), g) volatile organic compounds (VOC), and h) carbon monoxide (CO). The SSPs represented are SSP126, SSP245, SSP370 and SSP585. ASIA represents the emissions of most Asian countries with the exception of the Middle East, Japan, and the Former Soviet Union States, LAM, the emissions from Latin America and the Caribbean, MAF, the emissions from the Middle East and Africa, REF, the emissions from the reforming economics of Eastern Europe and the Former Soviet Union, and the Organization for Economic Co-operation and Development (OECD 90) countries as well as EU member states and candidates. Each bar graph represents an experiment that determined the GMST anomaly (the difference between the GMST in 2100 and the GMST during the 1850-1900 reference period) under the base conditions of each SSP, with the emissions of a species from one region set to preindustrial levels. The regions are ordered based on magnitude of the SSP585 anomaly.

This is expected because under these SSPs that represent scenarios with greater warmings, more of each greenhouse gas species is expected to be emitted, resulting in a greater GMST anomaly. Additionally, species generally seen as having a greater impact on the environment, such as CO_2 and methane (CH4), show the highest positive GMST anomaly (**Figures 1a, 1b**). The total was calculated from a separate experiment without emissions of a particular species, rather than being constructed from a linear addition of the other components. This allowed for the compounding, non-linear effects of various emissions removals to be considered.

Under each experiment, all the emissions are allowed to proceed as described in each SSP except for the target variable, which was held constant at its emissions from the 1850-1900 baseline. The difference between this experiment and the counterfactual FaIR experiment (where all variables follow the SSP conditions) represents the temperature response attributable to the target variable. FaIR, as part of its parameterizations, calculates the radiative forcing for different species using different parameterizations. This was necessary to capture the different spectroscopic properties of individual greenhouse gas species. For example, CO_2 is saturated in much of CO_2's absorption wavelengths but CH_4 is not. Due to these differences in saturation, the addition of one molecule of CH_4 to the atmosphere is more impactful than one molecule of CO_2, meaning that the atmosphere is more sensitive to CH_4 (7). FaIR represents these differences in saturation through different parameterizations, namely formulae describing the relationship between emissions and radiative forcing. These allow for our experiments to represent the differences in radiative forcing of each species along with emission differences.

Geographical Regions

First, we looked at the general trends among species and the impact of geographical regions on the GMST anomaly, or the predicted future warming of these variables. We calculated that CO_2, CH_4, black carbon (BC), volatile organic compounds (VOCs), and carbon monoxide (CO) cause warming, i.e. positive anomaly, for most regions, with sulfur, ammonia (NH_3), and nitric oxide and nitrogen dioxide (NO_X) showing a negative anomaly (**Figure 1**). For several of the species, the SSP370 "regional rivalry" experiment had a greater temperature anomaly than the SSP585 "fossil fuel development" experiment (**Table 1, Figures 1b-h**). Our analysis showed that the greater temperature anomaly in SSP585 is almost solely due to CO_2, which has an anomaly that is 1.08°C greater under SSP585 compared to SSP370 (**Figure 1a**). Our regional analysis showed that the region that represents the Asian countries with the exception of

https://doi.org/10.59720/24-067

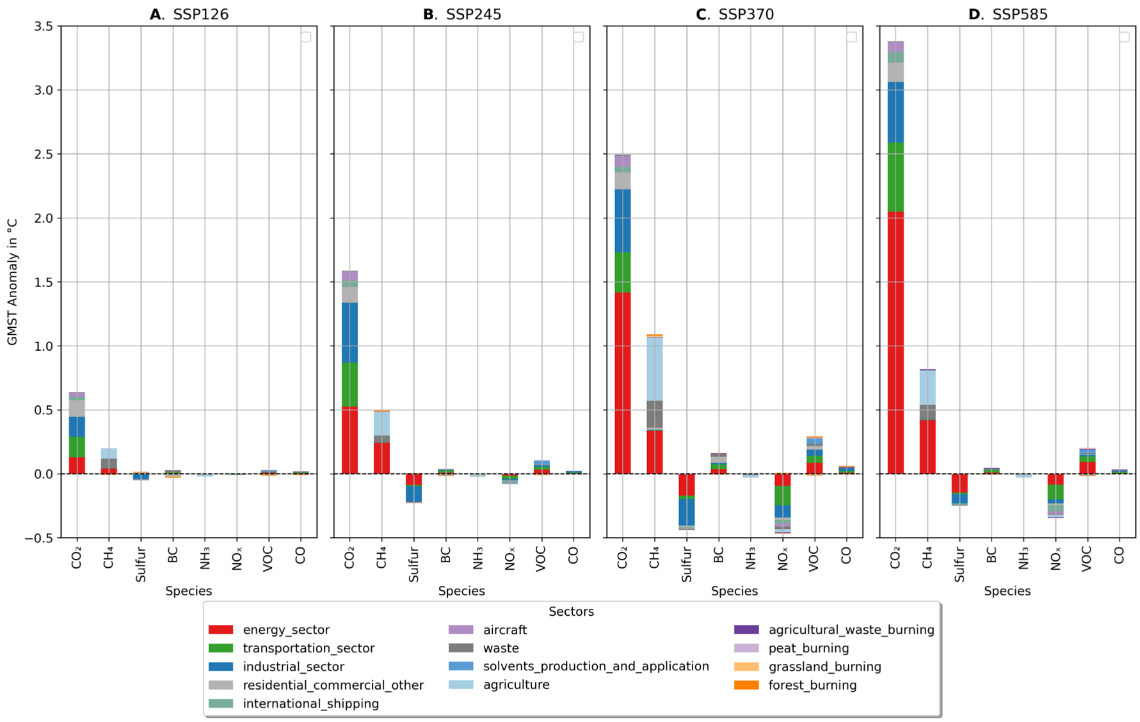

Figure 2: The predicted additive GMST anomaly in °C by greenhouse gas species and sector under four SSPs from the Finite Amplitude Impulse Response (FaIR) model. The SSPs represented are a) SSP126, b) SSP245, c) SSP370 and d) SSP585. Each bar graph represents the GMST anomaly (the difference between the GMST in 2100 and the GMST during the 1850-1900 reference period) for each greenhouse gas species in °C caused by each sector. Linear GMST anomalies are assumed for each sectoral experiment.

the Middle East, Japan, and the Former Soviet Union States (ASIA) is projected to contribute to the greatest positive GMST anomaly and is the most important region for six of the eight species we investigated. The Middle East and Africa (MAF) region is projected to be the greatest emitter for the other two species, CH_4 and BC (**Figures 1b, 1d**). In the CO_2 attribution experiment, the ASIA and MAF regions exhibit much more control over future warming than they have historically (**Figure 1a**). While the expected trend of greater warming under more extreme SSPs was noted here, this is not the case for the species with the second largest positive radiative forcing, CH_4. Under SSP370, CH_4 caused a larger GMST anomaly than under SSP585 (**Figure 1b**). While the MAF region was predicted to cause a similar amount of warming under SSP370 and SSP585 for CH_4, the ASIA region, under the instability scenario of SSP370, was projected to have an even greater warming effect (**Figure 1b**). The sulfur, BC, and VOC emissions showed a similar trend, where SSP370 had a greater magnitude anomaly (**Figures 1c, 1d, 1h**). For BC and CO, the Organization for Economic Co-operation and Development (OECD) region was projected to have lower emission levels from 2015-2100 than during the preindustrial period, resulting in a decrease in forcing in 2100 below the 1850-1900 baseline levels (**Figures 1d, 1h**). This resulted in a negative anomaly for otherwise net-positive GMST anomaly species because their emissions increased when restored to the 1850-1900 baseline.

Economic Sectors

Second, we looked at the impact of economic sectors on future GMST anomaly. With the assumption of linearity of the effects of sector-based reduction, we created a visualization of our species-sector attribution data, as well as the total impact of each species on GMST (**Figure 2**). The data very clearly shows a trend of increasing GMST anomaly magnitude from SSP126 to SSP585, although there are some deviations related to SSP370. Our analysis showed that CO_2 and CH_4 have a net warming effect, and sulfur has a net cooling effect. Other species have effects that are much smaller in magnitude and vary between positive and negative radiative forcings.

Averaged across the SSPs, CO_2 emissions from the energy and transportation sectors made up 64.39% of the CO_2 anomaly. Under SSP126, a pathway that assumes a large reduction in emissions, the emissions from the industrial and residential/commercial sectors were shown to have a relatively similar impact on GMST anomaly (**Figure 2a**). However, the percentage of the total anomaly accounted for by the industrial sector, increased from 12.97% in SSP585 to 32.44% in SSP126. The residential/commercial sectors' proportion of total anomaly similarly increased from 4.20% to 25.25% (**Figure 2**).

The warming due to CH_4, while positive like CO_2, resulted from emissions in different sectors, primarily in waste and agriculture, which together make up 62.74% of the anomaly averaged across the SSPs. Notably, the warming from CH_4 in SSP370 was projected to be larger than in SSP585, likely because of projected higher agricultural and waste emissions (**Figures 1, 2**). It is noteworthy that NO_X under SSP585 produced a cooling that is greater than that from sulfur emissions by 0.01°C (**Figure 2d**).

https://doi.org/10.59720/24-067

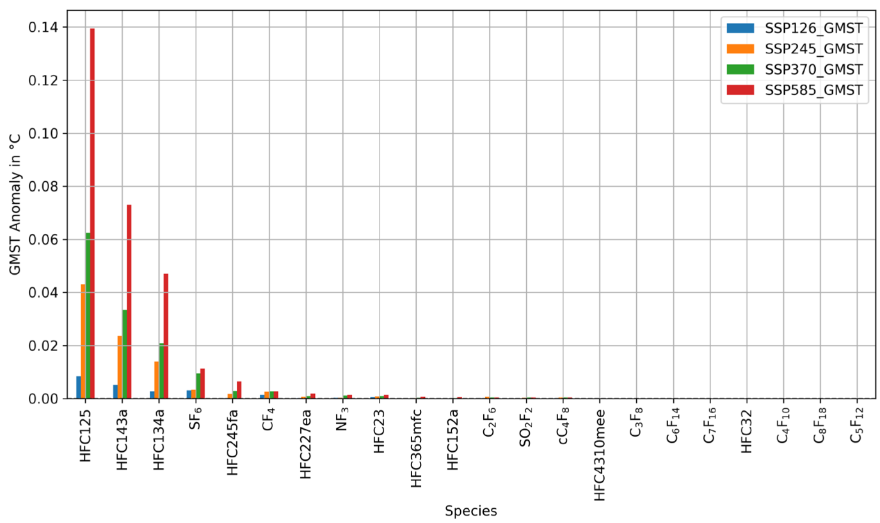

Figure 3: The predicted GMST anomaly in °C of fluorinated gas species under four SSPs from the Finite Amplitude Impulse Response (FaIR) model. The fluorinated gases are carbon tetrafluoride (CF_4), hexafluoroethane (C_2F_6), octafluoropropane (C_3F_8), octafluorocyclobutane (C_4F_8), perfluorobutane (C_4F_{10}), perfluoropentane (C_5F_{12}), perfluorohexane (C_6F_{14}), perfluoroheptane (C_7F_{16}), perfluorooctane (C_8F_{18}), nitrogen trifluoride (NF_3), sulfur hexafluoride (SF_6), and sulfuryl fluoride (SO_2F_2). The hydrofluorocarbons (HFCs) are pentafluoroethane (HFC125), 1,1,1,2-tetrafluoroethane (HFC134a), 1,1,1-trifluoroethane (HFC143a), 1,1-difluoroethane (HFC152a), 1,1,1,2,3,3,3-teptafluoropropane (HFC227ea), trifluoromethane or fluoroform (HFC23), 1,1,1,3,3,3-hexafluoropropane (HFC236fa), pentafluoropropane (HFC245fa), difluoromethane (HFC32), 1,1,1,3,3-pentafluorobutane (HFC365mfc), and 1,1,1,2,3,4,4,5,5,5-decafluoropentane (HFC4310mee). The SSPs represented are SSP126, SSP245, SSP370 and SSP585. The bar graphs show the GMST anomaly (the difference between the GMST in 2100 and the GMST during the 1850-1900 reference period) for each fluorinated gas species. All species shown have some anomaly on GMST change, even if not visible. The regions are ordered based on magnitude of the SSP585 anomaly.

Fluorinated Gases

Finally, we examined the future importance of a relatively new group of greenhouse gas species, fluorinated or F-gases, of which Hydrofluorocarbons (HFCs) make up a large part (**Figure 3**). These chemicals are potent greenhouse gases and are used as replacements for the ozone-depleting chlorofluorocarbons (CFCs), hydrochlorofluorocarbons (HCFCs), and halons, none of which fall under the label of F-gases (8). The impact of F-gases was shown to be outsized in comparison to their emissions. HFC125 (pentafluoroethane) showed a GMST anomaly of 0.14°C under SSP585, which is comparable to that of BC (which has the greatest anomaly in SSP370). The total impact of these F-gases, averaged across the SSPs, was shown to be 0.14°C, which is greater than that of BC, VOC, and CO individually. However, this effect was caused by a select few gases, primarily HFCs, while the other F-gases had near-negligible effects. For all the F-gases from 1,1,1,3,3,3-hexafluoropropane (Hfc236fa) to the right of the graph, the highest GMST anomaly in °C for all the SSPs is 0.000331 (**Figure 3**).

In our experiments, the average percent standard deviation over all SSPs was 28.76%, with an average percent deviation from the standard deviation of 1.05%. This shows a relatively constant range in temperature data across the experiments.

DISCUSSION

In this study, we hypothesized that various economic sectors, geographic regions, and greenhouse gas species could impact the future global mean surface temperature anomaly in ways that deviate from the historical and present norm. We aimed to address the projected GMST anomaly of specific economic sectors, geographic regions, and greenhouse gas species, to fill in the gaps of general analyses such as CMIP6. Our results demonstrate the larger GMST anomaly caused by SSP370 in non-CO_2 species, the larger impact of Africa and Asia on future radiative forcing, and the outsized impact of F-gases.

It is shown in our results that, while for CO_2, SSP585 is predicted to result in the largest net positive GMST anomaly, for many other species, the SSP370 "regional rivalry" scenario is expected to result in greater warming, showcasing the unique situation SSP370 describes. These greater warmings are surprising because SSP585 was constructed to produce a radiative forcing that is greater than SSP370 by 1.5 W/m2. We therefore conclude that, even in the higher emission scenarios, the role of CO_2 and other species is worthy of consideration and that emissions mitigation can still produce tangible and beneficial impacts. Furthermore, our results emphasize the climate risk posed by the SSP370 "regional rivalry" experiment in which geopolitical conflict results in a fragmented approach to emission reduction. This scenario is projected to result in very high emissions of species that result in the formation of secondary pollutants, such as acid deposition, particulate matter, and tropospheric ozone. Additionally, consistent with the continued industrialization of Asia, the Middle East, and Africa, these regions are predicted to play a much greater role in future warming than currently developed nations, represented by OECD (**Table 2**). This marks a reversal of the historical role of OECD nations being the primary emitters. As such, Asia, the Middle East, and Africa are the regions where existing and future decarbonization technology might bring about substantial benefit. Most notably, the ASIA and MAF regions make up 57.13% of the anomaly for CO_2 averaged across the SSPs, a drastic difference from the dominance of

https://doi.org/10.59720/24-067

the developed (OECD) nations over historical temperature change. In fact, for some species, setting OECD emissions back to preindustrial values reduces emissions, resulting in an anomaly opposite to the species' forcing. This means that under this scenario, sulfur, a negative radiative forcer, would have a positive anomaly, and CO_2, a positive radiative forcer, would have a negative anomaly.

The sector data for CO_2, the largest positive radiative forcer, shows that the transportation and energy sectors will have a steadily decreasing role over the GMST anomaly from SSP585 to SSP126, and GMST change due to the industrial sector will be more important. This suggests that the SSPs are accounting for the potential decarbonization of transportation and energy through renewable energy sources and electric vehicles but do not anticipate substantial decarbonization of industry, which would need to be an area of focus under the lower SSPs.

The expected strong role of agriculture and waste in the CH_4 anomaly contributes to its greater magnitude under SSP370 than under SSP585, consistent with the impact of geopolitical turmoil on increasing waste generation and decreasing the spread of more efficient agricultural practices. This analysis shows how important food production and waste removal are to the future climate. Of note is the much more prominent role of NO_x in future emissions compared to sulfur. This is interesting because, up until 2025, sulfur is the most important negative forcer, but the FaIR model predicts that this may not be the case in the future, with aerosol-producing NO_x being emitted more globally. The much more prominent role of NO_x in negative forcing compared to the historical period is notable due to its potential to increase the generation of PM 2.5 particulate matter and tropospheric ozone. In general, our results show that for many species, including the largest forcers of CH_4 and CO_2, concerted action across all sectors has the potential to be beneficial. Most notably, under the lower SSPs, CO_2 emission reductions in the energy, transportation, and industrial sectors are required. For CH_4, reductions in the agriculture, waste, and energy sectors are required.

Our data also shows the rapidly increasing importance of the newer man-made greenhouse gas species, many of which have radiative forcings greater than traditional greenhouse gas species. Pentafluoroethane (HFC125), 1,1,1-trifluoroethane (HFC143a), 1,1,1,2-tetrafluoroethane (HFC134a), and others are, under all the SSPs, contributing to a large amount of the global temperature anomaly at roughly 37.38% of the contribution of CH_4, making them the third largest positive forcer under SSP585. These gases, some of which are regulated under the Montreal Protocol, need to be further restricted due to their predicted outsized impact on the future GMST anomaly.

It is important to note that although the FaIR climate model is a fairly accurate emulator of CMIP6, it does not include a full treatment of all the climate components and their interactions in the manner of, or with the power of, an IPCC model and thus may not be as accurate in its projections (6). Additionally, since FaIR uses methodology similar to that used for CMIP6 by aggregating data from many different climate models, the arithmetic mean used in these calculations does not show the wide variety in GMST data that the individual CMIP6 models calculate. In our experiments, the average percent standard deviation over all SSPs was 28.76%, with an average percent deviation from this value of 1.05%, showing a relatively constant range in temperature data. While the manipulation of the emissions database completed for this paper allows for us to create "bridge" pathways between the SSPs, these are still based on the general SSP scenarios that reflect the best estimates of climate scientists and policy makers. Future work in this area could involve taking a more detailed look into the regional impacts of various sectors and species to move beyond the generalized global temperature anomaly used in this paper and thus better capture regional climate change.

Our research has shed light on the impact of specific regions, species, and sectors on the future GMST anomaly, showcasing the areas where emissions reduction is projected to be most required under the scenarios described by each SSP. Specifically, we found that the SSP370 scenario is projected to result in higher emissions for the majority of greenhouse gas species than the SSP585 scenario, potentially causing compounding issues related to pollution and acid deposition. We also found that under the lower SSP scenarios where significant emissions reductions are predicted, the industrial sector becomes a much larger emitter. We also found that Asia and Africa contribute a much larger percentage of future emissions and consequently warming, than seen in the historical period. Additionally, we found that anthropogenic F-gases are predicted to have a much larger impact on the GMST anomaly in the future relative to their historical impact, compared with the GMST anomaly of other major greenhouse gas species. Our research augments the SSPs by considering specific variables not represented in the general SSP scenarios, allowing us to ascertain the precise climate impacts of these factors. This study aims to pinpoint where emission reduction efforts should be concentrated to effectively and swiftly decarbonize the modern world. By utilizing our findings to initiate specific, data-driven climate policy, nations worldwide can work towards preserving a habitable planet for future generations.

MATERIALS AND METHODS

FaIR model

The FaIR model was accessed through a clone of the official GitHub repository (6). The primary inputs to this model are emissions of greenhouse gas species and short-lived climate forcers from the Reduced Complexity Model Intercomparison Project (RCMIP) annual means emission database (9). The RCMIP project aims to allow for the direct comparison of Reduced Complexity Models (RCMs) to the Earth Systems Models (ESMs) used in CMIP6 by providing standardized processes for these RCMs. We used the ERF relationships for CO_2, CH_4, and N_2O as defined by Etminan et al. in our FaIR experiments (10). For well-mixed greenhouse gas species not described in Etminan et al., the ERF was defined as a linear relationship of the change in concentration. For tropospheric ozone, and stratospheric ozone, we used the ERF coefficients identified by Stevenson et al., and Meinshausen et al. respectively (11, 12).

Using these ERF and RF parameters, as well as preindustrial concentrations of greenhouse gas species (preindustrial concentrations defined as the 1850-1900 average from the RCMIP inputs file), we ran several simulations in sequence, aiming to generate a full ensemble of CMIP6 data from the calibrated model (9). FaIR then further aggregated these simulations to create a summary dataframe with all the GMST data for each SSP, using the

https://doi.org/10.59720/24-067

Greenhouse Gas Species	Full Name
CO_2	Carbon dioxide
CH_4	Methane
BC	Black carbon
NH_3	Ammonia
NO_x	Nitrous oxides
VOC	Volatile organic compounds
CO	Carbon monoxide
HFC125	Pentafluoroethane
HFC143a	1,1,1-trifluoroethane
HFC134a	1,1,1,2-tetrafluoroethane

Table 3: The full names of the greenhouse gas species used for emission calculations in this paper.

RCMIP emissions to produce temperature anomalies that are equivalent to an analogous climate model experiment in CMIP6. To perform attribution experiments, the RCMIP input file was modified programmatically in place to generate emissions data for the FaIR algorithms, and thus any change to emissions data from this file would directly impact the GMST anomaly projections that FaIR would generate. We first ran the FaIR model using an unmodified RCMIP file to get the counterfactual experiment that we would then use as a baseline to define further anomalies.

Attribution experiment

For our attribution experiment, we used a backwards approach, and took the normal outputs from FaIR for each SSP and then selectively removed a specific aspect of emissions (13). This resulted in the FaIR GMST experiment giving a negative temperature anomaly for warming gases or regions and a positive temperature anomaly for cooling gases and regions. The warming resulting from a given species is then simply the difference between the two anomalies. We corrected for the negative anomaly by reversing the sign of the anomaly difference.

We defined the preindustrial concentrations as the average values from the 1850-1900 RCMIP data. Since the FaIR impulse response equations only used total emissions from each greenhouse gas species under a certain climate model and SSP, the RCMIP sector and region-based data were ignored by the climate model. Because the RCMIP emissions file is structured with emissions for a greenhouse gas species under a certain climate model repetitively broken down into its parts in later rows, we took the total emission rows of a greenhouse gas species from all the climate models and SSPs of RCMIP, subtracted the emissions from a specific sector and added the pre-industrial sector emissions, essentially removing this sector from FaIR's calculation of future emissions. This was only done for future emissions, and since the RCMIP file used data that ends in 2015, the columns representing emissions from 2016 to 2500 were modified. To perform the attribution tests on these specific datasets, we used pandas 2.0.3 (with Python 3.9.17) to automate the process, creating functions that systematically went through each greenhouse gas species used in FaIR and set its future emissions for each region and sector to preindustrial levels, thus creating an attribution for the variable (14). We also used the xarray (v2023.6.0) package and the Matplotlib (version 3.7.2) package for data analysis and plotting, respectively (15, 16). The attribution experiments were completed for each individual greenhouse gas species, each geographical region under each species, and each economic sector under each species (**Tables 2, 3**). The AFOLU (Agriculture, Forestry and Other Land Use) sector, as well as the Fossil and Industrial sector, were not included in the economic sector analysis because the various sectors shown are considered a part of these overarching labels in the RCMIP classification system.

Received: March 05, 2024
Accepted: April 24, 2024
Published: July 29, 2024

REFERENCES

1. Manabe, Syukuro and Richard T. Wetherald. "Thermal Equilibrium of the Atmosphere with a Given Distribution of Relative Humidity." *Journal of Atmospheric Sciences*, vol. 24, no. 3, May 1967, pp. 241-259. https://doi.org/10.1175/1520-0469(1967)024<0241:TEOTAW>2.0.CO;2
2. Anderson, Thomas R., et al. "CO2, the Greenhouse Effect and Global Warming: From the Pioneering Work of Arrhenius and Callendar to Today's Earth System Models." *Endeavour*, vol. 40, no. 3, Sept. 2016, pp. 178–187, https://doi.org/10.1016/j.endeavour.2016.07.002.
3. van Vuuren, D.P., et al. "The representative concentration pathways: an overview." *Climatic Change* vol. 109, no. 5, Aug. 2011, https://doi.org/10.1007/s10584-011-0148-z
4. Riahi, Keywan, et al. "The Shared Socioeconomic Pathways and Their Energy, Land Use, and Greenhouse Gas Emissions Implications: An Overview." *Global Environmental Change*, vol. 42, no. 42, Jan. 2017, pp. 153–168, https://doi.org/10.1016/j.gloenvcha.2016.05.009.
5. IPCC. "Sixth Assessment Report — IPCC." Ipcc.ch, *IPCC*, www.ipcc.ch/assessment-report/ar6/. Accessed 9 July 2023.
6. Leach, Nicholas J., et al. "FaIRv2.0.0: A Generalized Impulse Response Model for Climate Uncertainty and Future Scenario Exploration." *Geoscientific Model Development*, vol. 14, no. 5, 27 May 2021, pp. 3007–3036, https://doi.org/10.5194/gmd-14-3007-2021.
7. Taylor, K. E., and J. E. Penner. "Response of the Climate System to Atmospheric Aerosols and Greenhouse Gases." *Nature*, vol. 369, no. 6483, June 1994, pp. 734–737, https://doi.org/10.1038/369734a0.
8. Sovacool, Benjamin K., et al. "Climate Change and Industrial F-Gases: A Critical and Systematic Review of Developments, Sociotechnical Systems and Policy Options for Reducing Synthetic Greenhouse Gas Emissions." *Renewable and Sustainable Energy Reviews*, vol. 141, May 2021, p. 110759, https://doi.org/10.1016/j.rser.2021.110759.
9. Nicholls, Z., et al. "Reduced Complexity Model Intercomparison Project Phase 2: Synthesizing Earth System Knowledge for Probabilistic Climate Projections." *Earth's Future, vol.* 9, no. 6, June 2021, https://doi.org/10.1029/2020ef001900.
10. Etminan, M., et al. "Radiative Forcing of Carbon Dioxide, Methane, and Nitrous Oxide: A Significant Revision of the Methane Radiative Forcing." *Geophysical Research Letters*, vol. 43, no. 24, 27 Dec. 2016, pp. 12, 614–12,

https://doi.org/10.59720/24-067

623, https://doi.org/10.1002/2016gl071930.

11. Stevenson, D. S., et al. "Tropospheric Ozone Changes, Radiative Forcing and Attribution to Emissions in the Atmospheric Chemistry and Climate Model Intercomparison Project (ACCMIP)." *Atmospheric Chemistry and Physics*, vol. 13, no. 6, 15 Mar. 2013, pp. 3063–3085, https://doi.org/10.5194/acp-13-3063-2013.
12. Meinshausen, Malte, et al. "The RCP Greenhouse Gas Concentrations and Their Extensions from 1765 to 2300." *Climatic Change*, vol. 109, no. 1-2, 9 Aug. 2011, pp. 213–241, https://doi.org/10.1007/s10584-011-0156-z.
13. Jones, Gareth S., et al. "Uncertainties in the Attribution of Greenhouse Gas Warming and Implications for Climate Prediction." *Journal of Geophysical Research: Atmospheres*, vol. 121, no. 12, 27 June 2016, pp. 6969–6992, https://doi.org/10.1002/2015jd024337
14. McKinney, Wes. "Data Structures for Statistical Computing in Python." *Proceedings of the 9th Python in Science Conference*, 2010, pp. 56-61. http://doi.org/10.25080/Majora-92bf1922-00a
15. Hoyer, S., and J. Hamman. "Xarray: N-D Labeled Arrays and Datasets in Python." *Journal of Open Research Software*, vol. 5, no. 1, 2017, https://doi.org/10.5334/jors.148
16. Hunter, J. D. "Matplotlib: A 2D Graphics Environment." *Computing in Science & Engineering*, vol. 9, no. 3, 2007, pp. 90-95, https://doi.org/10.5281/zenodo.8118151